Published in final edited form as:

J Neurochem. 2015 October ; 135(2): 347–356. doi:10.1111/jnc.13242.

Microglial Hv1 proton channel promotes cuprizone-induced demyelination through oxidative damage

Junli Liu[*,†], **Daishi Tian**[†,‡], **Madhuvika Murugan**[†], **Ukpong B. Eyo**[†], **Cheryl F. Dreyfus**[§], **Wei Wang**[‡], and **Long-Jun Wu**[*,†]

[*]Cancer center, Union Hospital, Tongji Medical College, Huazhong University of Science and Technology, Wuhan, China

[†]Department of Cell Biology and Neuroscience, School of Arts and Sciences, Rutgers University, Piscataway, New Jersey, USA

[‡]Department of Neurology, Tongji Hospital, Tongji Medical College, Huazhong University of Science and Technology, Wuhan, China

[§]Department of Neuroscience and Cell Biology, Rutgers Robert Wood Johnson Medical School, Piscataway, New Jersey, USA

Abstract

NADPH oxidase (NOX)-dependent reactive oxygen species (ROS) production in inflammatory cells including microglia plays an important role in demyelination and free radical-mediated tissue injury in multiple sclerosis (MS). However, the mechanism underlying microglial ROS production and demyelination remains largely unknown. The voltage-gated proton channel, Hv1, is selectively expressed in microglia and is required for NOX-dependent ROS generation in the brain. In the present study, we sought to determine the role of microglial Hv1 proton channels in a mouse model of cuprizone-induced demyelination, a model for MS. Following cuprizone exposure, wild-type mice presented obvious demyelination, decreased myelin basic protein expression, loss of mature oligodendrocytes, and impaired motor coordination in comparison to mice on a normal chow diet. However, mice lacking Hv1 ($Hv1^{-/-}$) are partially protected from demyelination and motor deficits compared with those in wild-type mice. These rescued phenotypes in $Hv1^{-/-}$ mice in cuprizone-induced demyelination is accompanied by reduced ROS production, ameliorated microglial activation, increased oligodendrocyte progenitor cell (NG2) proliferation, and increased number of mature oligodendrocytes. These results demonstrate that the Hv1 proton channel is required for cuprizone-induced microglial oxidative damage and subsequent demyelination. Our study suggests that the microglial Hv1 proton channel is a unique target for controlling NOX-dependent ROS production in the pathogenesis of MS.

Address correspondence and reprint requests to Dr Long-Jun Wu, Department of Cell Biology and Neuroscience, Rutgers University, 604 Allison Road, Piscataway, NJ 08854, USA. lwu@dls.rutgers.edu.

conflict of interest disclosure

The authors have no conflict of interest to declare.

Keywords

cuprizone; demyelination; microglia; multiple sclerosis; oligodendrocytes; voltage-gated proton channel Hv1

Multiple sclerosis (MS) is a heterogeneous inflammatory demyelinating disease, which causes chronic neurological disability beginning in early-to-mid adult life (Hauser and Oksenberg 2006). The cuprizone intoxication model, an established toxicant-induced chronic demyelination model, is characterized by apoptosis of primary oligodendrocytes and demyelinating lesions particularly in the corpus callosum (CC) that mimics some aspects of MS (Blakemore and Franklin 2008). Cuprizone-induced demyelination is accompanied by overwhelming glial activation, such as microgliosis and astrogliosis (Remington *et al.* 2007; Gudi *et al.* 2011). However, microglial function in demyelination and underlying mechanisms are not understood.

Oxidative damage from reactive oxygen species (ROS) has been reported to account for pathological features of MS, including demyelination, oligodendrocyte apoptosis, and astrocyte dysfunction (Haider *et al.* 2011). Mechanistically, ROS causes damage to biological macromolecules, such as polyunsaturated fatty acids in membrane lipids, proteins, and DNA/RNA in MS lesions (Liu *et al.* 2001; Diaz-Sanchez *et al.* 2006). Inflammation-associated oxidative burst in activated microglia and macrophages is considered to be the major source of ROS in MS (Miller *et al.* 2013). Indeed, NADPH oxidase (NOX)-dependent ROS production in inflammatory cells plays an important role in demyelination and free radical-mediated tissue injury in the pathogenesis of MS (Fischer *et al.* 2012). Thus, reducing NOX-related oxidative stress may represent a reasonable strategy to ameliorate axonal damage in MS lesions.

Hv1 (encoded by gene *Hvcn1*), a novel voltage-gated proton channel, is ideally suited to the task of charge compensation for NOX activation by sensing both voltage and pH gradients (Ramsey *et al.* 2006; Sasaki *et al.* 2006; Wu 2014b). Deletion or inhibition of Hv1 greatly reduced NOX-dependent ROS production in leukocytes and bone marrow cells (Okochi *et al.* 2009; Ramsey *et al.* 2009). Recently, we identified that Hv1 was selectively expressed in microglia and was required for NOX-dependent ROS generation in the brain (Wu *et al.* 2012). The study showed that mice lacking Hv1 ($Hv1^{-/-}$) were protected from NOX-mediated neuronal death and brain damage after ischemic stroke. In the present study, we investigated the role of microglial Hv1 proton channel in demyelination after cuprizone exposure and whether Hv1 is a unique target for controlling NOX-dependent ROS production in the pathogenesis of MS.

Materials and methods

Animals and cuprizone treatment

Wild-type (WT) C57BL/6 mice, $CX3CR1^{GFP/+}$ mice, $Hv1^{-/-}$ mice, and $Hv1^{-/-}$-$CX3CR1^{GFP/+}$ mice were used in the present study. All mice were purchased from Jax laboratory except $Hv1^{-/-}$ mice (Wu *et al.* 2012; Eyo *et al.* 2015). Mice were used in accordance with institutional guidelines as approved by the animal care and use committee

at Rutgers University. All mice were housed in a temperature and humidity-controlled environment with a 12-h light–dark cycle. The details of cuprizone demyelination model were described in our previous study (VonDran *et al.* 2011; Fulmer *et al.* 2014). In brief, 8-week-old male mice were fed 0.2% (w/w) cuprizone (Bis(cyclohexanone)oxaldihydrazone, Sigma; St. Louis, MO, USA) combined with powdered chow or control feed for 4 weeks (Harlan Teklad). Food containing cuprizone was changed every 2 days for 4 weeks. Mice used for behavioral testing were given a cuprizone diet for 6 weeks and immediately after cuprizone withdrawal normal chow was replaced for an additional 14 days as a recovery phase.

Rotarod test

Motor co-ordination and balance were evaluated using a rotarod apparatus (Med Associates Inc, St. Albans, VT, USA), which consisted of a motor-driven rotating rod equipped with variable speeds. The mice were evaluated on the rotarod three times a day for three consecutive days with the rotation set between 8 and 80 rpm. The duration for which each animal stayed on the rod (holding time) was recorded. The data presented for motor function are means from the 9 trials from the 3 consecutive days (3 trials per day). There was no significant individual daily difference in the motor function deficit in the rotarod performance tests.

Oil red O staining

Mice were anesthetized and perfused intracardially with phosphate-buffered saline followed by 4% paraformaldehyde, and the brains were treated with graded concentrations of sucrose (15–30%) for cryoprotection. Cryosections of 15 μm thickness were generated. Since cuprizone administration causes varying degrees of demyelination within the CC (Stidworthy *et al.* 2003), we chose comparable sections at approximately the same anatomical co-ordinates for staining and observed at the middle of the caudal CC, overlying the hippocampus. Frozen sections were incubated in distilled water for 1 min followed by 2 min incubation in 100% propylene glycol (Polyscientific; Bayshore, NY, USA) whereupon the sections were transferred to Oil Red O for 36 h at (20–25°C) room temperature. Sections were incubated for 1 min in 85% propylene glycol, lightly stained with hematoxylin, and mounted with gelatin mounting medium.

Immunofluorescence

For immunofluorescence staining, cryosections were incubated for 1 h in blocking buffer consisting of 5% goat serum, Tris-buffered saline (TBS), and 0.1% Triton X-100. Before staining, the fixed sections were washed three times with phosphate-buffered saline for 10 min each. The following primary antibodies were used for immunostaining: rabbit anti-glial fibrillary acidic protein (GFAP) (Chemicon, Temecula, CA, USA, 1 : 500), mouse anti-myelin basic protein (MBP) (Covance, Dedham, MA, USA, 1 : 2000), rabbit anti-Iba-1 (Wako, Richmond, VA, USA, 1 : 500), mouse anti-CC1 (Abcam, Cambridge, MA, USA, 1 : 50), and mouse anti-8 hydroxyguanosine (8-OHG, Abcam, 1 : 200). The primary antibodies were diluted in blocking buffer, applied individually to tissue sections, and incubated overnight at 4°C after which the tissue sections were washed three times for 5 min each with

TBS and were incubated for 60 min in Alexa 594-labeled goat anti-mouse antibodies (for MBP and 8-OHG antibodies) or Alexa 488-labeled goat anti-rabbit antibodies (for GFAP) at a dilution of 1 : 500. The sections were washed three times for 5 min each in TBS before further observation.

BrdU incorporation and detection

To identify the proliferation of oligodendrocyte progenitor cells (OPCs), mice were injected intraperitoneally with 200 mg/kg bromodeoxyuridine (BrdU; Sigma) at 4 and 2 h before killing (Armstrong *et al.* 2002). Brain sections from BrdU-injected mice were treated to permeabilize the tissue and denature the DNA, and were then incubated overnight with the following primary antibodies: rabbit polyclonal anti-NG2 antibody (1 : 200, Chemicon) and mouse monoclonal anti-BrdU antibody (1 : 50). The secondary antibodies (1 : 500 dilutions) used were Alexa 488-labeled goat anti-mouse antibodies for BrdU detection and Alexa 594-labeled goat anti-rabbit antibodies for NG2 detection. The sections were then washed and mounted to be imaged. For BrdU counting, three coronal sections per animal were analyzed with five randomly selected images within each area of interest (CC).The total numbers of all $BrdU^+$ cells and $BrdU^+$ $NG2^+$ cells (oligodendrocyte progenitors) per field were counted.

Western blot

Corpus callosum (CC) samples were homogenized in lysis buffer, and the homogenates were centrifuged at 7000 *g* for 15 min at 4°C. The supernatants were collected and the protein concentration was determined by the Bradford method. Equal amounts of protein sample (30 μg) were separated on 10% sodium dodecyl sulfate polyacrylamide gels, transferred to polyvinylidene difluoride membranes, and blocked in 5% non-fat dry milk buffer. The membranes were then incubated with the following antibodies: rabbit anti-GFAP (Chemicon, 1 : 500), mouse anti-MBP (Covance, 1 : 2000), rabbit anti-Iba-1 (Wako, 1 : 500) diluted in blocking buffer overnight at 4°C. Rabbit anti-Glyceraldehyde 3-phosphate dehydrogenase polyclonal antibody (Sigma, 1 : 2000) was detected on immunoblots as a loading control for protein quantification. Following washes, the membranes were incubated with horseradish peroxidase-conjugated anti-rabbit or anti-mouse IgG (Santa Cruz Biotechnology, Santa Cruz, CA, USA, 1 : 2000) at (20–25°C) room temperature for 1 h and developed with enhanced chemiluminescence detection reagents as a color substrate. The membranes were scanned at 600 dpi, and the resulting digital images were analyzed quantitatively. The integrated optical density (OD) of the signals was semi-quantified and expressed as the ratio of OD from the indicated markers to OD from Glyceraldehyde 3-phosphate dehydrogenase.

Quantifications and statistical analysis

All cell counts and intensity analyses were performed blind to the experimental treatment and data were expressed as mean ± SEM. All statistical tests were performed using GraphPad Prism (GraphPad software, La Jolla, CA, USA). The group comparison was performed with two-tailed *t*-test and Student-Newman-Keuls method ($_{ANOVA}$). $p < 0.05$ were considered to be statistically significant.

Results

$Hv1^{-/-}$ mice show reduced demyelination and less impaired motor co-ordination after cuprizone exposure

Cuprizone intoxication causes demyelination in the brain, particularly in the CC region (Steelman *et al.* 2012; Gudi *et al.* 2014). To study the function of microglial Hv1 proton channel in cuprizone-induced demyelination, we used Oil Red O staining to visualize lipid-rich myelin debris and compared the demyelination in WT and Hv1 knockout mice ($Hv1^{-/-}$). In WT mice fed with cuprizone for 4 weeks, obvious demyelination in the CC with a vast amount of lipid debris was observed in comparison to mice on a normal chow diet (Fig. 1a and b). However, the number of deposited myelin debris was reduced in cuprizone-treated $Hv1^{-/-}$ mice as compared to those in the WT group (Fig. 1b). These results suggest that $Hv1^{-/-}$ mice are protected from cuprizone-induced demyelination.

Demyelination in the CC after cuprizone exposure leads to impairments in motor function in mice (Franco-Pons *et al.* 2007; Iwasa *et al.* 2014). Since $Hv1^{-/-}$ mice had attenuated cuprizone-induced demyelination visualized by Oil Red O staining, we wanted to examine whether this can be translated into behavioral phenotypes. To this end, we monitored motor coordination and balance using an accelerated rotarod test after mice were fed with cuprizone for 6 weeks. Consistent with previous studies, we found that cuprizone treatment significantly reduced the mean running time on the rotarod test (Fig. 1c, $p < 0.01$), suggesting that cuprizone intoxication indeed impairs motor coordination. Interestingly, when we compared $Hv1^{-/-}$ mice with WT mice after cuprizone treatment, $Hv1^{-/-}$ mice stayed for a longer time on the rotarod apparatus than WT mice (Fig. 1c, $p < 0.05$). These results indicate that $Hv1^{-/-}$ mice are protected from cuprizone-induced motor deficits. We also examined motor behaviors in mice at 2 weeks of recovery under normal chow after 6 weeks of cuprizone feeding. Even after 2 weeks of recovery from cuprizone treatment, $Hv1^{-/-}$ mice still had better motor coordination than WT mice (Fig. 1c, $p < 0.01$). Therefore, the attenuation of cuprizone-induced motor deficits by Hv1 deficiency is long-lasting. Together, our results show that a deficiency in the Hv1 proton channel protected mice from cuprizone intoxication, exhibiting better functional motor recovery consistent with reduced demyelination.

Reduced microglial activation in $Hv1^{-/-}$ mice after cuprizone exposure

Both microgliosis and astrogliosis were closely correlated with demyelination in the cuprizone model (Remington *et al.* 2007; Gudi *et al.* 2011). Since Hv1 is selectively expressed in microglia in the brain, the reduced demyelination and motor deficits after cuprizone intoxication in $Hv1^{-/-}$ mice (Fig. 1) could be associated with microglial activation. To test this idea, we examined the microgliosis in cuprizone-induced demyelination. Using $CX3CR1^{GFP/+}$ mice in which microglia are labeled with green fluorescent protein (GFP) (Jung *et al.* 2000), we observed a massive accumulation of GFP-positive microglia in bilateral regions of the CC after 4 weeks of cuprizone. In $CX3CR1^{GFP/+}$ mice lacking Hv1, the microgliosis was attenuated as compared to the WT group after cuprizone exposure (Fig. 2a and b). To further quantify the degree of microglial activation, western blot analysis was performed to investigate the expression of microglial

marker Iba1. Consistently, we found that the Iba1 protein expression was dramatically up-regulated in WT mice (around 5 fold) and the Iba1 up-regulation was compromised in $Hv1^{-/-}$ mice after cuprizone exposure (Fig. 2e and f, $p < 0.05$). Therefore, microgliosis and microglial activation after cuprizone treatment were attenuated in $Hv1^{-/-}$ mice compared with WT mice.

We further analyzed astrogliosis during cuprizone-induced demyelination immunostaining and western blot using anti-GFAP, a commonly used marker for astrocytes. Under control condition with normal chow, there was no significant difference of GFAP immunostaining in the CC between WT mice and $Hv1^{-/-}$ mice. After 4 weeks of cuprizone feeding, the fluorescence intensity of GFAP was markedly increased. However, there was no significant difference in astrogliosis between the $Hv1^{-/-}$ and WT groups after cuprizone treatment (Fig. 2c and d). These results were further confirmed by western blot analysis of GFAP expression. GFAP was up-regulated in the groups exposed to cuprizone compared to their respective control group on a normal diet, but no statistical difference was observed between $Hv1^{-/-}$ and WT mice (Fig. 2e and f). Thus, the deficiency of the Hv1 proton channel reduces microgliosis but not astrogliosis after cuprizone treatment.

Attenuated microglia-derived ROS production in the corpus callosum in $Hv1^{-/-}$ mice after cuprizone exposure

Hv1 is known to be engaged in NOX-dependent ROS production in microglia (Wu *et al.* 2012; Wu 2014b). Given the critical role of ROS in cuprizone-induced demyelination (Gudi *et al.* 2014; Praet *et al.* 2014), we next tested the idea that Hv1-mediated ROS production might account for the attenuated demyelination phenotype we observed in $Hv1^{-/-}$ mice. To characterize ROS production in the CC, we used an 8-OHG antibody to detect oxidized nucleic acids resulting from cellular ROS damage (Nunomura *et al.* 1999). Four weeks after cuprizone diet, the intensity of 8-OHG immunoreactive signals increased significantly in the CC compared with that in control mice (Fig. 3a and c). The 8-OHG signals were mainly localized in GFP^+ microglial cells indicating that microglia are the major ROS-producing cells in the CC after cuprizone intoxication. In $Hv1^{-/-}$ mice, we found that the quantified intensity of 8-OHG immunoreactive signals and the co-localization of 8-OHG signal and GFP were substantially reduced compared with WT mice after 4 weeks of cuprizone treatment (Fig. 3c, $p < 0.05$). These results suggest that microglial Hv1 proton channels indeed contribute to microglial ROS production after cuprizone exposure.

Increased number of $NG2^+$-$BrdU^+$ cells and suppressed MBP reduction in $Hv1^{-/-}$ mice after cuprizone exposure

NG2 is a proteoglycan present on the OPC that increase in number in response to the cuprizone lesion and are important for remyelination after cuprizone-induced injury (Mason *et al.* 2000). Recent studies showed that NG2 cell proliferation after cuprizone demyelination is sensitive to ROS damage (Husain and Juurlink 1995; Back *et al.* 1998). Therefore, we wanted to evaluate the impact of Hv1 proton channel deficiency on the proliferation of NG2 cells after cuprizone treatment. To this end, NG2 immunostaining was performed to identify OPCs and BrdU incorporation was used to study cell proliferation in the CC. Consistent with previous studies (Deverman and Patterson 2012; Sachs *et al.* 2014),

the number of proliferating OPCs, as measured by BrdU labeling, was largely increased after 4 weeks of cuprizone treatment in WT mice (Fig. 4a and b). Interestingly, we found that there was a significant increase in the number of total BrdU positive cells as well as NG2-BrdU double positive cells in $Hv1^{-/-}$ mice than in those in WT mice (Fig. 4b and c, $p < 0.05$). Together, these results show an increase in NG2 proliferation in $Hv1^{-/-}$ mice, suggesting that the reduced cuprizone-induced damage in $Hv1^{-/-}$ mice might be partially due to the remyelination from the increased number of $NG2^{+}$-$BrdU^{+}$ cells.

Increased $NG2^{+}$-$BrdU^{+}$ cells in $Hv1^{-/-}$ mice compared with those in WT mice may lead to enhanced remyelination and mature oligodendrocytes after cuprizone-induced injury (Mason *et al.* 2000). To begin to test this idea, MBP immunoreactivity and levels were first analyzed at 4 weeks following cuprizone intoxication. Strong MBP-positive immunostaining was observed in the CC of both WT and $Hv1^{-/-}$ control groups. In the cuprizone exposure group, there was a remarkable reduction in MBP immunoreactivity (Fig. 5a and b). However, the cuprizone-induced MBP decrease was ameliorated in $Hv1^{-/-}$ group compared to the WT group (Fig. 5a and b). Consistently, western blot analysis confirmed that MBP expression was significantly reduced after cuprizone treatment, but the reduction was partially reversed in $Hv1^{-/-}$ mice (Fig. 5c and d, $p < 0.05$). In line with the ameliorated MBP reduction, we also found that there were significant more mature oligodendroctyes in $Hv1^{-/-}$ mice than in WT mice after cuprizone treatment (Fig. 5e and f, $p < 0.05$). Therefore, these results demonstrate a possible enhanced remyelination due to the increased number of mature oligodendrocytes in $Hv1^{-/-}$ mice, suggesting that the microglial Hv1 proton channel aggravates remyelination in cuprizone intoxication.

Discussion

In the present study, we found that $Hv1^{-/-}$ mice have reduced microglial accumulation, ROS production, increased NG2 proliferation, and are partially protected from demyelination and motor deficits after cuprizone exposure. These results suggest that microglial Hv1 proton channels may promote cuprizone-induced demyelination through ROS production. Our study is the first to explore microglial Hv1 function in the pathogenesis of demyelination and extends previous evidence of oxidative injury in MS (Haider *et al.* 2011; van Horssen *et al.* 2011; Fischer *et al.* 2012).

Microglia, the resident hematopoietic cells in the central nervous system (CNS), participate in the regulation of immune responses due to their ability to present antigens and secrete immunoregulatory factors such as neurotrophins, chemokines, cytokines, and ROS (Voss *et al.* 2012; Eyo and Wu 2013). It has been debated whether microglia play a harmful or beneficial role in demyelination/remyelination during MS. On one hand, microglia can exert neuroprotective effects through the expression of anti-inflammatory molecules, phagocytosis of debris, and tissue repair. On the other hand, there is evidence demonstrating a detrimental role for microglia. For example, mice with ablated microglia were protected in an experimental model of autoimmune enchephalomyelitis (Heppner *et al.* 2005). In addition, microglia can recruit and reactivate T cells in the CNS and release many detrimental molecules such as proteases, inflammatory cytokines, and free radicals, which then contribute toxicity to bystanders like neurons and glial cells (Rawji and Yong 2013). In line

with the harmful role of microglia in the MS, we found increased microgliosis and microglial activation associated with myelin loss and OPC loss in mice after cuprizone exposure. In $Hv1^{-/-}$ mice, there was attenuated microglial activation and reduced demyelination, suggesting that microglial Hv1 promotes cuprizone-induced demyelination.

Recently, several studies provided evidence for oxidative damage of oligodendrocytes and dystrophic axons in early stages of active MS lesions (Haider *et al.* 2011; Fischer *et al.* 2012). For instance, mitochondrial pathology and focal axonal degeneration were initiated by the macrophage-mediated production of reactive oxygen and nitrogen species (ROS and RNS). Neutralization of the ROS and RNS could effectively reverse axonal degeneration and thus protect tissue injury in MS (van Horssen *et al.* 2011). Here, we found that 8-OHG expression, a marker of ROS, was up-regulated in activated microglia at week 4 after cuprizone diet, indicating increased ROS production after demyelination. ROS production by microglia occurred primarily by NOX activation and required the Hv1 proton channel (Wu 2014a). Through providing compensating charge or relieving intracellular acidosis for NOX, Hv1 was coupled to NOX-dependent pH regulation, membrane depolarization, or ROS production in a variety of cells, including neutrophils (El Chemaly *et al.* 2010), B cells (Capasso *et al.* 2010), and eosinophils (Zhu *et al.* 2013). Consistently, in $Hv1^{-/-}$ mice, there was decreased ROS production in activated microglia compared with that in WT mice after cuprizone treatment. These results demonstrate that the Hv1 proton channel is critical in demyelination-associated ROS production in microglia.

Although extensive evidence implicates increased ROS production in inflammatory demyelinating diseases, the underlying mechanisms of ROS-dependent myelin loss are not yet clear. Firstly, it has been reported that ROS could directly induce the apoptosis of oligodendrocytes, thereby leading to demyelination in MS (Griot *et al.* 1990; Witherick *et al.* 2010). Secondly, OPC such as NG2 cells appear to be significantly more sensitive to oxidative stress compared to mature oligodendrocytes (Husain and Juurlink 1995; Back *et al.* 1998). Therefore, ROS may directly target NG2 cells and thus limit CNS repair and remyelination. Thirdly, ROS also exerts direct effects on the lipid and protein components of myelin through peroxidation, and degrade MBP through the production of matrix metalloproteinases (Witherick *et al.* 2010). In our present study, we found that ROS was largely produced by activated microglia after cuprizone exposure through the Hv1 proton channel. In $Hv1^{-/-}$ mice after cuprizone treatment, decreased ROS production was associated with attenuated demyelination shown by Oil red staining, increased proliferating NG2 cells, and suppressed MBP reduction. As cuprizone intoxication is associated with oligodendrocytes death, loss in myelin proteins as well as progenitors maturation. The rescue of reduced MBP levels or the number of mature oligodendrocytes in $Hv1^{-/-}$ mice could be due to the reduction in dying oligodendrocytes, or the decrease in demyelination, or the increase in the number of $BrdU^{+}$ NG2 progenitor cells. Future studies are needed to dissect the exact mechanism underlying Hv1 function in cuprizone-induced MBP alterations. Nevertheless, our results indicate that the Hv1-dependent microglial ROS promotes demyelination and hinders remyelination in cuprizone-induced injury.

In summary, our current study provides a mechanistic insight into microglia-induced myelin loss after cuprizone exposure. Microglial cells produce several cytotoxic mediators,

including ROS, that may contribute directly or indirectly to the selective oligodendrocyte/myelin injury and loss. We found that the microglial Hv1 proton channel promotes cuprizone-induced demyelination and reduced proliferating NG2 related remyelination through ROS production. Identification of microglial Hv1 channels as a key factor in ROS production could serve as a novel potential therapeutic target for patients with demyelinating diseases including MS.

Acknowledgments

This work is supported by National Institute of Health (R01NS088627), American Heart Association (11SDG7340011), Michael J. Fox Foundation, National Multiple Sclerosis Society (RG4257B4/1), and National Natural Science Foundation of China (81101766, 81171157).

All experiments were conducted in compliance with the ARRIVE guidelines.

Abbreviations used

8-OHG	8 hydroxyguanosine
BrdU	bromodeoxyuridine
CC	corpus callosum
CNS	central nervous system
Ctrl	control
Cupz	cuprizone
GAPDH	Glyceraldehyde 3-phosphate dehydrogenase
GFAP	glial fibrillary acidic protein
MBP	myelin basic protein
MS	multiple sclerosis
NOX	NADPH oxidase
OD	optical density
OPCs	oligodendrocyte progenitor cells
ROS	reactive oxygen species
WT	wild-type.

References

Armstrong RC, Le TQ, Frost EE, Borke RC, Vana AC. Absence of fibroblast growth factor 2 promotes oligodendroglial repopulation of demyelinated white matter. J. Neurosci. 2002; 22:8574–8585. [PubMed: 12351731]

Back SA, Gan X, Li Y, Rosenberg PA, Volpe JJ. Maturation-dependent vulnerability of oligodendrocytes to oxidative stress-induced death caused by glutathione depletion. J. Neurosci. 1998; 18:6241–6253. [PubMed: 9698317]

Blakemore WF, Franklin RJ. Remyelination in experimental models of toxin-induced demyelination. Curr. Top. Microbiol. Immunol. 2008; 318:193–212. [PubMed: 18219819]

Capasso M, Bhamrah MK, Henley T, et al. HVCN1 modulates BCR signal strength via regulation of BCR-dependent generation of reactive oxygen species. Nat. Immunol. 2010; 11:265–272. [PubMed: 20139987]

Deverman BE, Patterson PH. Exogenous leukemia inhibitory factor stimulates oligodendrocyte progenitor cell proliferation and enhances hippocampal remyelination. J. Neurosci. 2012; 32:2100–2109. [PubMed: 22323722]

Diaz-Sanchez M, Williams K, DeLuca GC, Esiri MM. Protein co-expression with axonal injury in multiple sclerosis plaques. Acta Neuropathol. 2006; 111:289–299. [PubMed: 16547760]

El Chemaly A, Okochi Y, Sasaki M, Arnaudeau S, Okamura Y, Demaurex N. VSOP/Hv1 proton channels sustain calcium entry, neutrophil migration, and superoxide production by limiting cell depolarization and acidification. J. Exp. Med. 2010; 207:129–139. [PubMed: 20026664]

Eyo UB, Wu LJ. Bi-directional microglia-neuron communication in the healthy brain. Neural. Plast. 2013; 2013:456857. [PubMed: 24078884]

Eyo UB, Gu N, De S, Dong H, Richardson JR, Wu LJ. Modulation of microglial process convergence toward neuronal dendrites by extracellular calcium. J. Neurosci. 2015; 35:2417–2422. [PubMed: 25673836]

Fischer MT, Sharma R, Lim JL, et al. NADPH oxidase expression in active multiple sclerosis lesions in relation to oxidative tissue damage and mitochondrial injury. Brain. 2012; 135:886–899. [PubMed: 22366799]

Franco-Pons N, Torrente M, Colomina MT, Vilella E. Behavioral deficits in the cuprizone-induced murine model of demyelination/remyelination. Toxicol. Lett. 2007; 169:205–213. [PubMed: 17317045]

Fulmer CG, VonDran MW, Stillman AA, Huang Y, Hempstead BL, Dreyfus CF. Astrocyte-derived BDNF supports myelin protein synthesis after cuprizone-induced demyelination. J. Neurosci. 2014; 34:8186–8196. [PubMed: 24920623]

Griot C, Vandevelde M, Richard A, Peterhans E, Stocker R. Selective degeneration of oligodendrocytes mediated by reactive oxygen species. Free Radic. Res. Commun. 1990; 11:181–193. [PubMed: 1965721]

Gudi V, Skuljec J, Yildiz O, et al. Spatial and temporal profiles of growth factor expression during CNS demyelination reveal the dynamics of repair priming. PLoS ONE. 2011; 6:e22623. [PubMed: 21818353]

Gudi V, Gingele S, Skripuletz T, Stangel M. Glial response during cuprizone-induced de- and remyelination in the CNS: lessons learned. Front Cell Neurosci. 2014; 8:73. [PubMed: 24659953]

Haider L, Fischer MT, Frischer JM, et al. Oxidative damage in multiple sclerosis lesions. Brain. 2011; 134:1914–1924. [PubMed: 21653539]

Hauser SL, Oksenberg JR. The neurobiology of multiple sclerosis: genes, inflammation, and neurodegeneration. Neuron. 2006; 52:61–76. [PubMed: 17015227]

Heppner FL, Greter M, Marino D, et al. Experimental autoimmune encephalomyelitis repressed by microglial paralysis. Nat. Med. 2005; 11:146–152. [PubMed: 15665833]

van Horssen J, Witte ME, Schreibelt G, de Vries HE. Radical changes in multiple sclerosis pathogenesis. Biochim. Biophys. Acta. 2011; 1812:141–150. [PubMed: 20600869]

Husain J, Juurlink BH. Oligodendroglial precursor cell susceptibility to hypoxia is related to poor ability to cope with reactive oxygen species. Brain Res. 1995; 698:86–94. [PubMed: 8581507]

Iwasa K, Yamamoto S, Takahashi M, Suzuki S, Yagishita S, Awaji T, Maruyama K, Yoshikawa K. Prostaglandin F2alpha FP receptor inhibitor reduces demyelination and motor dysfunction in a cuprizone-induced multiple sclerosis mouse model. Prostaglandins Leukot. Essent. Fatty Acids. 2014; 91:175–182. [PubMed: 25224839]

Jung S, Aliberti J, Graemmel P, Sunshine MJ, Kreutzberg GW, Sher A, Littman DR. Analysis of fractalkine receptor CX(3)CR1 function by targeted deletion and green fluorescent protein reporter gene insertion. Mol. Cell. Biol. 2000; 20:4106–4114. [PubMed: 10805752]

Liu JS, Zhao ML, Brosnan CF, Lee SC. Expression of inducible nitric oxide synthase and nitrotyrosine in multiple sclerosis lesions. Am. J. Pathol. 2001; 158:2057–2066. [PubMed: 11395383]

Mason JL, Jones JJ, Taniike M, Morell P, Suzuki K, Matsushima GK. Mature oligodendrocyte apoptosis precedes IGF-1 production and oligodendrocyte progenitor accumulation and

differentiation during demyelination/remyelination. J. Neurosci. Res. 2000; 61:251–262. [PubMed: 10900072]

Miller E, Wachowicz B, Majsterek I. Advances in antioxidative therapy of multiple sclerosis. Curr. Med. Chem. 2013; 20:4720–4730. [PubMed: 23834174]

Nunomura A, Perry G, Pappolla MA, Wade R, Hirai K, Chiba S, Smith MA. RNA oxidation is a prominent feature of vulnerable neurons in Alzheimer's disease. J. Neurosci. 1999; 19:1959–1964. [PubMed: 10066249]

Okochi Y, Sasaki M, Iwasaki H, Okamura Y. Voltage-gated proton channel is expressed on phagosomes. Biochem. Biophys. Res. Commun. 2009; 382:274–279. [PubMed: 19285483]

Praet J, Guglielmetti C, Berneman Z, Van der Linden A, Ponsaerts P. Cellular and molecular neuropathology of the cuprizone mouse model: clinical relevance for multiple sclerosis. Neurosci. Biobehav. Rev. 2014; 47C:485–505. [PubMed: 25445182]

Ramsey IS, Moran MM, Chong JA, Clapham DE. A voltage-gated proton-selective channel lacking the pore domain. Nature. 2006; 440:1213–1216. [PubMed: 16554753]

Ramsey IS, Ruchti E, Kaczmarek JS, Clapham DE. Hv1 proton channels are required for high-level NADPH oxidase-dependent superoxide production during the phagocyte respiratory burst. Proc. Natl Acad. Sci. USA. 2009; 106:7642–7647. [PubMed: 19372380]

Rawji KS, Yong VW. The benefits and detriments of macrophages/microglia in models of multiple sclerosis. Clin. Dev. Immunol. 2013; 2013:948976. [PubMed: 23840244]

Remington LT, Babcock AA, Zehntner SP, Owens T. Microglial recruitment, activation, and proliferation in response to primary demyelination. Am. J. Pathol. 2007; 170:1713–1724. [PubMed: 17456776]

Sachs HH, Bercury KK, Popescu DC, Narayanan SP, Macklin WB. A new model of cuprizone-mediated demyelination/remyelination. ASN Neuro. 2014; 6:1–16.

Sasaki M, Takagi M, Okamura Y. A voltage sensor-domain protein is a voltage-gated proton channel. Science. 2006; 312:589–592. [PubMed: 16556803]

Steelman AJ, Thompson JP, Li J. Demyelination and remyelination in anatomically distinct regions of the corpus callosum following cuprizone intoxication. Neurosci. Res. 2012; 72:32–42. [PubMed: 22015947]

Stidworthy MF, Genoud S, Suter U, Mantei N, Franklin RJ. Quantifying the early stages of remyelination following cuprizone-induced demyelination. Brain Pathol. 2003; 13:329–339. [PubMed: 12946022]

VonDran MW, Singh H, Honeywell JZ, Dreyfus CF. Levels of BDNF impact oligodendrocyte lineage cells following a cuprizone lesion. J. Neurosci. 2011; 31:14182–14190. [PubMed: 21976503]

Voss EV, Skuljec J, Gudi V, Skripuletz T, Pul R, Trebst C, Stangel M. Characterisation of microglia during de- and remyelination: can they create a repair promoting environment? Neurobiol. Dis. 2012; 45:519–528. [PubMed: 21971527]

Witherick J, Wilkins A, Scolding N, Kemp K. Mechanisms of oxidative damage in multiple sclerosis and a cell therapy approach to treatment. Autoimmune Dis. 2010; 2011:164608. [PubMed: 21197107]

Wu LJ. Microglial voltage-gated proton channel Hv1 in ischemic stroke. Transl Stroke Res. 2014a; 5:99–108. [PubMed: 24323712]

Wu LJ. Voltage-gated proton channel HV1 in microglia. Neuroscientist. 2014b; 20:599–609. [PubMed: 24463247]

Wu LJ, Wu G, Akhavan Sharif MR, Baker A, Jia Y, Fahey FH, Luo HR, Feener EP, Clapham DE. The voltage-gated proton channel Hv1 enhances brain damage from ischemic stroke. Nat. Neurosci. 2012; 15:565–573. [PubMed: 22388960]

Zhu X, Mose E, Zimmermann N. Proton channel HVCN1 is required for effector functions of mouse eosinophils. BMC Immunol. 2013; 14:24. [PubMed: 23705768]

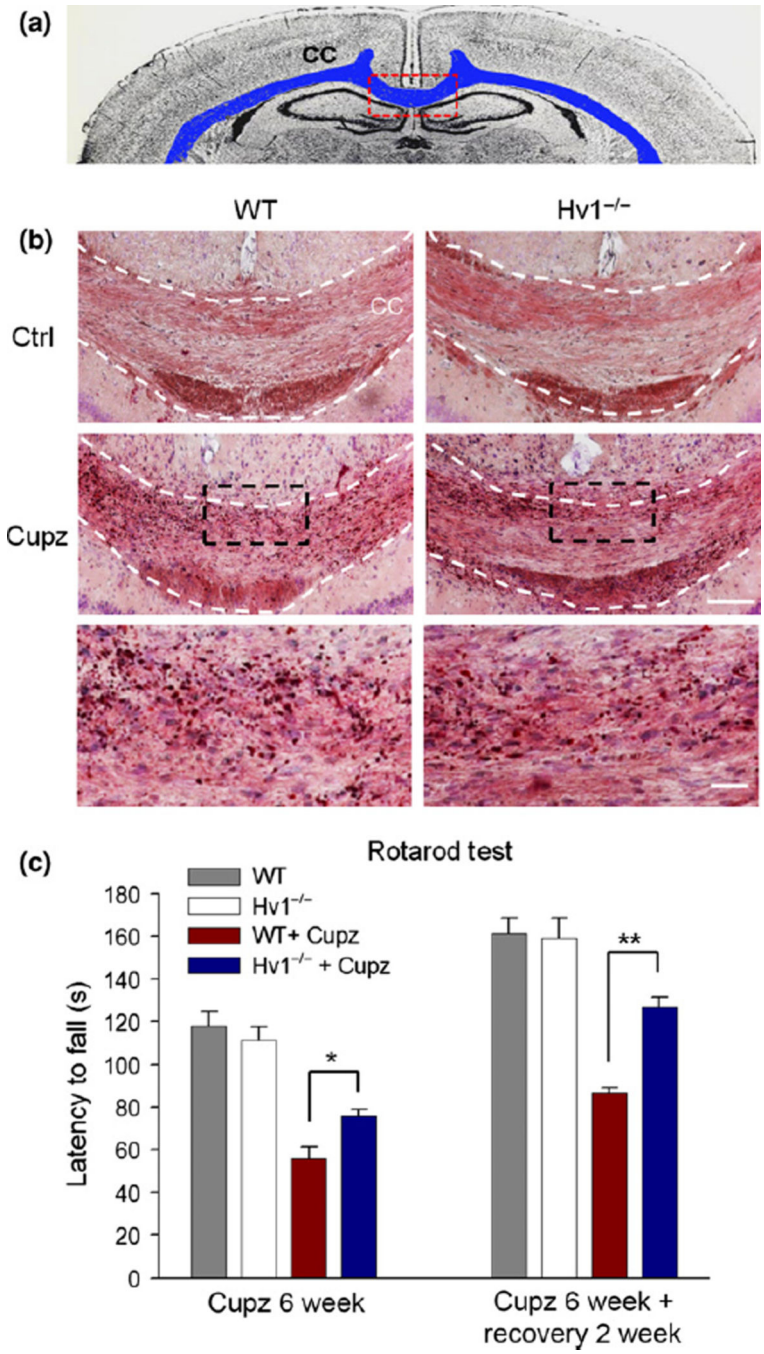

Fig. 1.

Hv1 deficiency reduces demyelination and motor co-ordination deficits after cuprizone exposure. (a) A diagram showing the corpus callosum (CC, in blue) in the mouse brain. Dotted red line delineated the CC area for the analysis of Oil Red O staining. (b) Reduced demyelination in $Hv1^{-/-}$ mice after cuprizone treatment compared with that in wild-type (WT) mice. Oil Red O staining of the mouse CC was used to visualize accumulation of lipid-rich myelin debris and the degree of demyelination after 4w cuprizone treatment (Cupz) (n = 3 mice each group). The regions in black rectangular boxes were magnified in

the lower panel. (c) $Hv1^{-/-}$ mice showed better motor coordination than WT mice after cuprizone treatment in rotarod test. The mean latency to fall in rotarod test was decreased in mice after cuprizone treatment (n = 10 mice for cuprizone treatment groups) compared with control group with saline normal chow (n = 5 mice for control groups). However, $Hv1^{-/-}$ mice with cuprizone ($Hv1^{-/-}$ + Cupz, n = 10 mice) performed better than WT mice (WT + Cupz, n = 10 mice). After recovery with normal chow for 2 weeks, $Hv1^{-/-}$ mice still have better motor coordination than WT mice. Data are means ± SEM, *$p < 0.05$, **$p < 0.01$, unpaired t-test. In this figure and the following figures, CC regions are demarcated with white dashed lines.

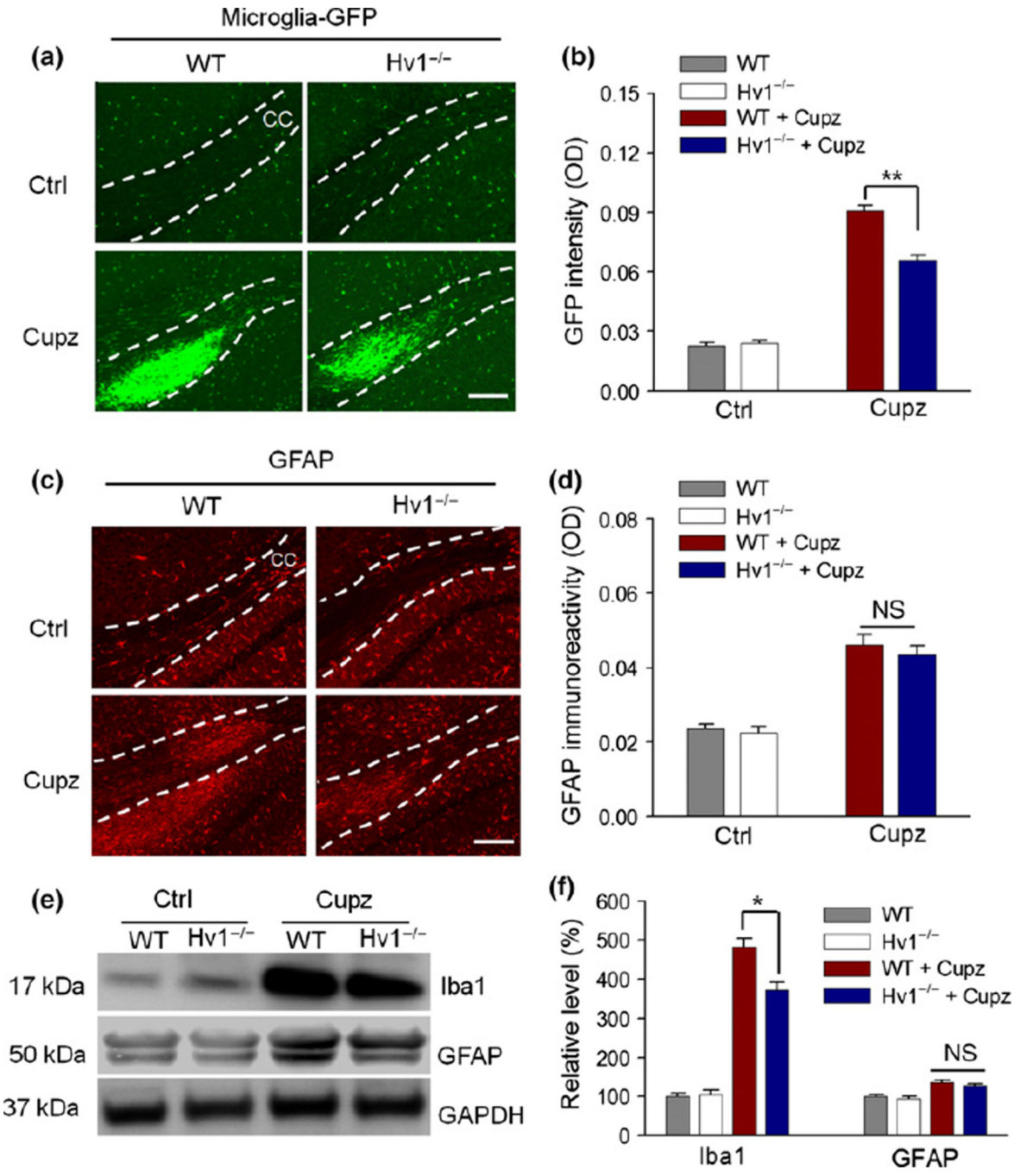

Fig. 2.

Hv1 deficiency reduces microgliosis in response to cuprizone intoxication. (a) Reduced microgliosis in $Hv1^{-/-}$ mice compared with wild-type (WT) mice after 4w cuprizone treatment. Microglia were labeled with GFP using $CX3CR1^{GFP/+}$ mice. Cuprizone-induced microgliosis was observed as a dense GFP signal in lateral corpus callosum (CC) which was reduced in $Hv1^{-/-}$ mice. Scale bar, 200 μm. (b) The summarized graph of average GFP intensity showing the reduced microgliosis in $Hv1^{-/-}$ mice compared with WT mice after 4w cuprizone treatment ($n = 3$ mice for each group). $^{**}p < 0.01$. (c) Cuprizone treatment

increased astrocyte activation shown as glial fibrillary acidic protein (GFAP) staining. However, there is no difference of GFAP staining between WT and $Hv1^{-/-}$ mice after cuprizone treatment. Scale bar, 200 μm. (d) The summarized graph average optical density (OD) of GFAP immunoreactivity showing similar GFAP staining in WT and $Hv1^{-/-}$ mice after cuprizone treatment (n = 3 mice for each group). n.s., no significance. (e) Western blots of Iba-1 and GFAP level in the CC from control and cuprizone-treated WT and $Hv1^{-/-}$ mice. Cuprizone-induced increase in Iba1 level was reduced in $Hv1^{-/-}$ mice compared with WT mice. (f) Summarized data showing that cuprizone-induced Iba1 increase were comprised in $Hv1^{-/-}$ mice compared WT mice. Each bar is shown as a ratio of its own optical density to that of Glyceraldehyde 3-phosphate dehydrogenase (GAPDH) expression (n = 3 mice for each group). *$p < 0.05$.

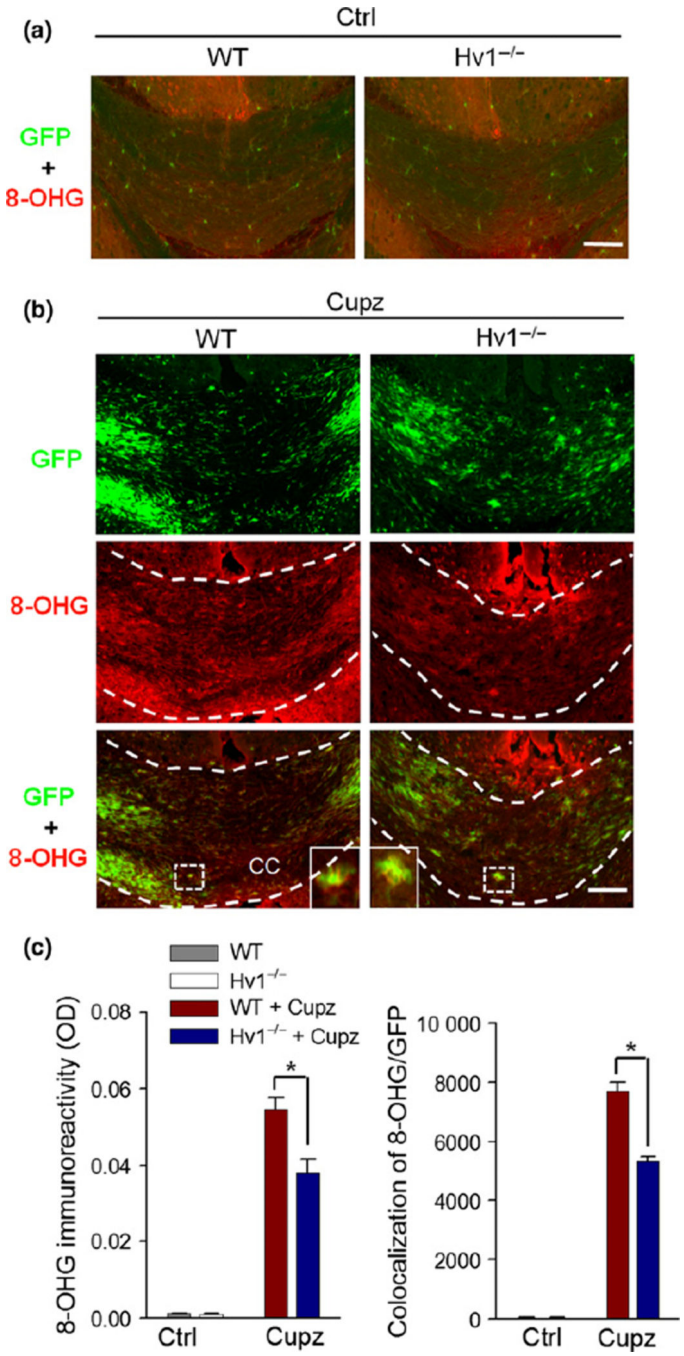

Fig. 3.

Hv1 deficiency attenuated microglial ROS production after cuprizone treatment. (a) Representative images showing microglial ROS production examined by 8 hydroxyguanosine (8-OHG) staining in GFP positive microglia ($CX3CR1^{GFP/+}$). Under control condition with normal chow feeding, there is very limited 8-OHG positive GFP microglia in the corpus callosum (CC) from either wild-type (WT) or $Hv1^{-/-}$ mice. Scale bar, 200 μm. (b) After 4-week cuprizone exposure, 8-OHG immunoreactivity was dramatically increased in the CC. However, the cuprizone-induced increase in 8-OHG

staining was attenuated in $Hv1^{-/-}$ mice compared with WT mice. Insets are the enlarged images shown for a single microglia that is 8-OHG positive. Scale bar, 200 μm. (c) The bar graphs summarizes the 8-OHG immunoreactivity (left) and the colocalization pixels of 8-OHG signals with GFP microglia (right) per field of CC region ($n = 3$ mice for each group) showing the reduced 8-OHG microglia in $Hv1^{-/-}$ mice compared with those in WT mice after cuprizone treatment. $*p < 0.05$.

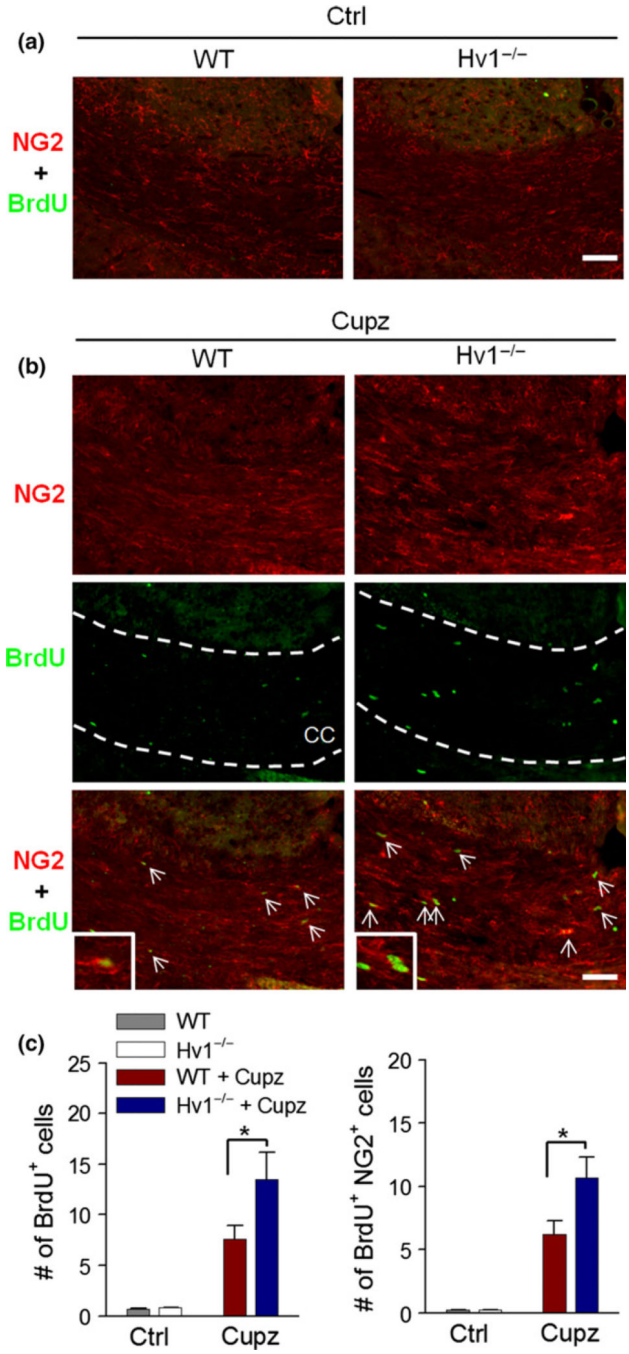

Fig. 4.

Hv1 deficiency increases the proliferation of NG2 cells after cuprizone treatment. (a) Representative images showing double staining of NG2 and bromodeoxyuridine (BrdU) in control condition with normal chow feeding. There are very limited BrdU+ cells in the corpus callosum (CC) from either wild-type (WT) or $Hv1^{-/-}$ mice. Scale bar, 200 μm. (b) Representative images of NG2 and BrdU immunoreactivity in the CC to study the proliferation of NG2 cells in WT and $Hv1^{-/-}$ mice after cuprizone treatment. Arrows point to $BrdU^{+}$ $NG2^{+}$ cells. Insets are respective enlarged images of $BrdU^{+}$ $NG2^{+}$ cells. Scale bar,

200 μm. (c) The summarized bar graphs showing the number of $BrdU^+$ cells (left) and $BrdU^+NG2^+$ cells (oligodendrocyte progenitors, right) in the CC region in WT and $Hv1^{-/-}$ mice from control- and cuprizone-treated group ($n = 4$ mice in each group). *$p < 0.05$.

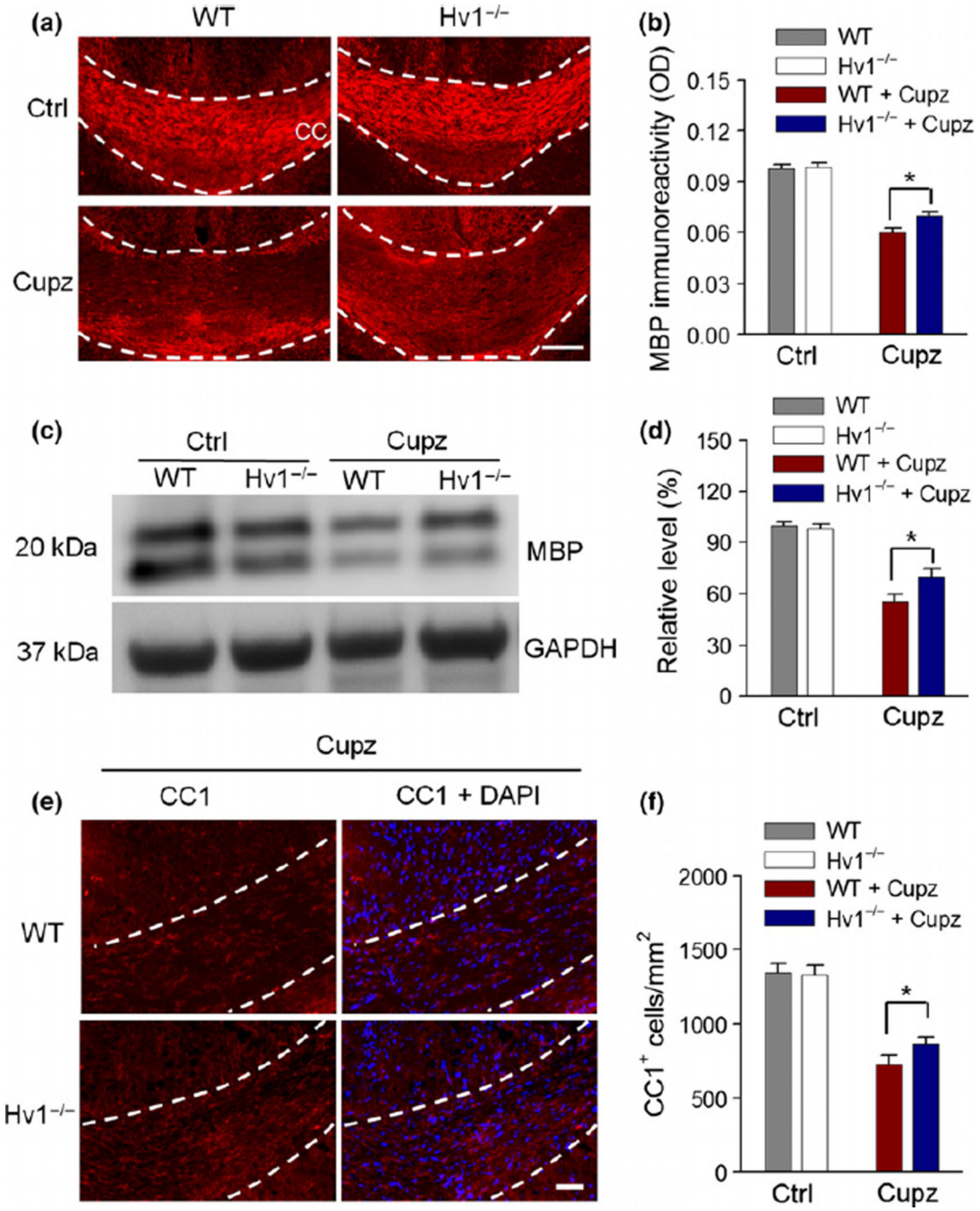

Fig. 5.

Hv1 deficiency attenuates the cuprizone-induced reduction in the myelin basic protein (MBP). (a) Representative corpus callosum (CC) sections of wild-type (WT) and $Hv1^{-/-}$ mice from control- and cuprizone-treated groups were stained with an antibody for MBP. (b) The summarized data showing that the MBP immunoreactivity were reduced after cuprizone treatment. However, the reduction in MBP staining was attenuated in $Hv1^{-/-}$ mice compared with WT mice ($n = 3$ mice for each group). *$p < 0.05$. Scale bar, 200 μm. (c) Western blot analysis of MBP in the CC from WT and $Hv1^{-/-}$ mice in control and cuprizone-treated

groups. (d) The summarized bar graph showing densitometric analysis of the MBP immunoreactive bands normalized with Glyceraldehyde 3-phosphate dehydrogenase (GAPDH) as internal/ loading control ($n = 3$ mice for each group). *$p < 0.05$. (e) Representative images of mature oligodendrocyte examined by CC1 immunostaining in the CC to study the loss of adult oligodendrocytes exposure to cuprizone. DAPI staining (blue) was used for cell counting. Scale bar, 200 μm. (f) The summarized bar graphs showing the number of CC1-positive cells per field of CC region in WT and $Hv1^{-/-}$ mice from control- and cuprizone-treated group. The cuprizone-induced loss of mature oligodendrocytes was significantly attenuated in $Hv1^{-/-}$ mice compared with those in WT group after intoxication ($n = 3$ mice in each group). *$p < 0.05$.